Supplementary Data

Communicated to: *Dalton Trans*
Manuscript Type: Article
Manuscript id: DT-ART-06-2013-051641-R1

New Ruthenium(II) Arene Complexes of Anthracenyl-appended Diazacycloalkanes: Effect of Ligand Intercalation and Hydrophobicity on DNA and Protein Binding and Cleavage and Cytotoxicity

Mani Ganeshpandian,[a] Rangasamy Loganathan,[a] Eringathodi Suresh,[b] Anvarbatcha Riyasdeen,[c] Mohammad Abdulkadher Akbarsha[d,e] and Mallayan Palaniandavar[a,*]

[a]*Department of Chemistry, Central University of Tamil Nadu, Thiruvarur 610 004, India*
[b]*Analytical Science Discipline, Central Salt and Marine Chemical Research Institute, Bhavnagar 364 002, India*
[c]*Department of Animal Science, Bharathidasan University, Tiruchirappalli – 620 024, Tamilnadu, India*
[d]*Mahatma Gandhi-Doerenkamp Center for Alternatives to use of Animals in Life Science Education, Bharathidasan University, Tiruchirappalli, 620024, Tamilnadu, India*
[e]*Visiting Scientist, Department Food and Nutrition, King Saud University, Riyadh, Kingdom of Saudi Arabia*

*Author to whom correspondence should be addressed *e-mail*: palaniandavar@cutn.ac.in, palanim51@yahoo.com

Results and Discussion

Energy transfer between BSA and 4

When the complex **4** exhibits protein binding affinity higher than **1** – **3**, fluorescence resonance energy transfer (FRET) from protein to complex **4** has been verified by overlapping the UV-Vis absorption spectrum of **4** with the fluorescence emission spectrum of BSA (**Figure 10**), according to the Förster theory of non radioactive energy transfer.[1] This is also useful for calculating the distance (r_0) between the BSA (donor) and the bound complex (acceptor) by using the equation:

$$E = 1 - (F/F_o) = \frac{R_0^6}{R_0^6 + r_0^6} \qquad \text{eqn 1}$$

where E is the energy transfer efficiency and R_0 is the critical distance between donor and acceptor when the transfer efficiency is 50% and can be calculated from the following equation:

$$R_0^6 = 8.8 \times 10^{-25} K^2 N^{-4} \Phi J \qquad \text{eqn 2}$$

where K^2 is the spatial orientation factor (2/3) related to the donor and acceptor of dipoles, N is the average refractive index of medium (1.36) in the wavelength range where the spectral overlap is significant, Φ is the fluorescence quantum yield of the donor $(0.15)^2$ and J is the spectral overlap integral of fluorescence emission spectrum of the donor and the absorption spectrum of the acceptor, which can be calculated by the equation:

$$J = \frac{\sum F(\lambda)\, \varepsilon(\lambda)\, \lambda^4 \Delta\lambda}{\sum F(\lambda)\, \Delta\lambda} \qquad \text{eqn 3}$$

where F(λ) is the fluorescence intensity of the donor in the range from λ to λ + Δλ, and ε is the molar absorption coefficient of the acceptor at wavelength λ. From equations 1 - 3 the values of J (1.814×10^{-15} cm^3 M^{-1}), E (0.56), R_0 (1.68 nm) and r_0 (1.93 nm) have been calculated.

References

1. T. H. Wang, Z. M. Zhao, B. Z. Wei, L. Zhang and L. Ji, *J. Mol. Struct*., 2010, **970**, 128–133.

2. M. Y. Tian, X. F. Zhang, L. Xie, J. F. Xiang, Y. L. Tang and C. Q. Zhao, *J. Mol. Struct*., 2008, **892**, 20–24.

Table S1. Electronic absorption spectral properties and electrochemical data of Ru(II) Complexes

Complex	λ_{max}, nm (ε, $M^{-1}cm^{-1}$)[a]	$E_{1/2}$ (V)[d] DPV[e]
[Ru(η^6-benzene)(L1)Cl]$^+$ **1**[b]	312 (689), 371 (512)	0.344
[Ru(η^6-benzene)(L2)Cl]$^+$ **2**[c]	251 (55478) 354 (6912), 372 (9812), 393 (8800),	0.337
[Ru(η^6-*p*-cymene)(L1)Cl]$^+$ **3**[b]	312 (1020), 369 (784)	0.341
[Ru(η^6- *p*-cymene)(L2)Cl]$^+$ **4**[c]	252 (55478) 354 (7509), 372 (10691), 393 (9766)	0.326

[a]In 1% ACN/5 mM Tris-HCl/50 mM NaCl buffer (pH 7.1). [b]Concentration, 1×10^{-3} M. [c]Concentration, 12×10^{-5} M. [d]Measured *vs* non-aqueous Ag/Ag^+ reference electrode; add 544 mV [300 mV, Ag/Ag^+ to SCE + 244 mV, SCE to SHE] to convert to standard hydrogen electrode (SHE); Fc/Fc^+ couple, $E_{1/2}$, 0.042 (DPV), Scan rate 50 mV s^{-1}; Supporting electrolyte, *Tetra-N*-butylammonium perchlorate (0.1 mol dm^{-3}); Complex concentration, 1 mmol dm^{-3}; [e]Differential Pulse Voltammetry, scan rate 5 mVs^{-1}; pulse height 25 mV.

Table S2. Theoretically calculated selected interatomic distances [Å] and bond angles [deg] for complexes **1**, **2**, **3** and **4**

1		**2**	
Bond Distance **[Å]**		Bond Distance **[Å]**	
Ru(1)-N(1)	2.1775	Ru(1)-N(1)	2.2113
Ru(1)-N(2)	2.2147	Ru(1)-N(2)	2.1956
Ru(1)-Cl(1)	2.4257	Ru(1)-Cl(1)	2.4335
Ru(1)-C(10)	2.2805	Ru(1)-C(1)	2.3010
Ru(1)-C(9)	2.2847	Ru(1)-C(2)	2.3005
Ru(1)-C(4)	2.2738	Ru(1)-C(3)	2.3326
Ru(1)-C(5)	2.2963	Ru(1)-C(4)	2.2931
Ru(1)-C(7)	2.2953	Ru(1)-C(5)	2.2985
Ru(1)-C(12)	2.3284	Ru(1)-C(6)	2.2752
Bond Angle [deg]		Bond Angle [deg]	
N(1)-Ru(1)-N(2)	71.844	N(1)-Ru(1)-N(2)	73.686
N(1)-Ru(1)-Cl(1)	88.499	N(1)-Ru(1)-Cl(1)	88.254
N(2)-Ru(1)-Cl(1)	88.131	N(2)-Ru(1)-Cl(1)	88.189
3		**4**	
Bond Distance **[Å]**		Bond Distance **[Å]**	
Ru(1)-N(1)	2.1914	Ru(1)-N(1)	2.2080
Ru(1)-N(2)	2.2314	Ru(1)-N(2)	2.2258
Ru(1)-Cl(1)	2.4350	Ru(1)-Cl(1)	2.4349
Ru(1)-C(11)	2.3308	Ru(1)-C(6)	2.3612
Ru(1)-C(16)	2.3114	Ru(1)-C(14)	2.2673
Ru(1)-C(8)	2.2665	Ru(1)-C(24)	2.2875
Ru(1)-C(5)	2.3299	Ru(1)-C(11)	2.3753
Ru(1)-C(4)	2.2666	Ru(1)-C(12)	2.3028
Ru(1)-C(10)	2.2723	Ru(1)-C(7)	2.2648
Bond Angle [deg]		Bond Angle [deg]	
N(1)-Ru(1)-N(2)	71.295	N(1)-Ru(1)-N(2)	73.305
N(1)-Ru(1)-Cl(1)	88.058	N(1)-Ru(1)-Cl(1)	88.017
N(2)-Ru(1)-Cl(1)	88.628	N(2)-Ru(1)-Cl(1)	87.133

Table S3 Energy of HOMO and LUMO molecular orbitals

Complexes	HOMO (eV)	LUMO (eV)	Energy gap (eV)
[Ru(η^6-benzene)(L1)Cl]$^+$ **1**	-9.3371	-5.2706	4.0665
[Ru(η^6-benzene)(L2)Cl]$^+$ **2**	-7.7236	-4.9569	2.7667
[Ru(η^6-*p*-cymene)(L1)Cl]$^+$ **3**	-9.0277	-5.0031	4.0246
[Ru(η^6- *p*-cymene)(L2)Cl]$^+$ **4**	-7.6100	-4.8254	2.7846

Table S4 CD parameters for the interaction of Calf Thymus DNA with ruthenium(II) complexes

Complex	CD Spectral band[a] wavelength (nm)	
	Positive band	Negative band
CT DNA	275	245
[Ru(η^6-benzene)(L1)Cl]$^+$ **1**	272	241
[Ru(η^6-benzene)(L2)Cl]$^+$ **2**	276	246
[Ru(η^6-*p*-cymene)(L1)Cl]$^+$ **3**	271	240
[Ru(η^6- *p*-cymene)(L2)Cl]$^+$ **4**	275	247

[a]Measurement made at 1/R = [Ru]/[DNA] value of 1 for complexes **1** – **4**; concentration of DNA solutions = 2.5×10^{-5} M. Cell path length, 1 cm.

Table S5. Cleavage of SC pUC19 DNA (40 μM) by complexes **1 – 4** (150 μM**)** in the absence of an external agent

Lane	Reaction conditions	Form (%)	
		SC	NC
1	DNA	91.3	8.7
2	DNA + **1**	47.1	52.9
3	DNA + **2**	46.8	53.2
4	DNA + **3**	46.5	53.5
5	DNA + **4**	45.7	54.3
6	DNA + $[Ru(\eta^6\text{-}p\text{-cym})Cl_2]_2$	70.6	29.4
7	DNA + $RuCl_3{\cdot}3H_2O$	85.1	14.9

Table S6. Concentration-dependent DNA (40 μM) cleavage by complex **4** (20 – 100 μM) in a buffer containing 5 mM Tris HCl/50 mM NaCl in the presence of H_2O_2 (30 μM) at 37 ^oC.

Lane	Reaction conditions	Form (%)	
		SC	NC
1	DNA	94.5	5.5
2	DNA + H_2O_2	91.3	8.7
3	DNA + H_2O_2 + **4** (20 μM)	87.6	12.4
4	DNA + H_2O_2 + **4** (40 μM)	62.2	37.8
5	DNA + H_2O_2 + **4** (60 μM)	49.3	50.7
6	DNA + H_2O_2 + **4** (80 μM)	18.1	81.9
7	DNA + H_2O_2 + **4** (100 μM)	8.6	91.4

Table S7. Quenching parameters of the interaction of complexes **1** – **4** with BSA at two temperatures (298 and 308 K)

Complexes	Temp (K)	$K_{sv} \times 10^4$ (L mol^{-1})	$k_q \times 10^{13}$ (L mol^{-1} s^{-1})
[(η^6-benzene)Ru(L1)Cl]$^+$ **1**	298	4.82	0.77
	308	4.66	0.75
[(η^6-benzene)Ru(L2)Cl]$^+$ **2**	298	9.94	1.60
	308	9.05	1.45
[(η^6-*p*-cymene)Ru(L1)Cl]$^+$ **3**	298	6.22	1.00
	308	5.91	0.93
[(η^6-*p*-cymene)Ru(L2)Cl]$^+$ **4**	298	11.63	1.87
	308	10.87	1.76

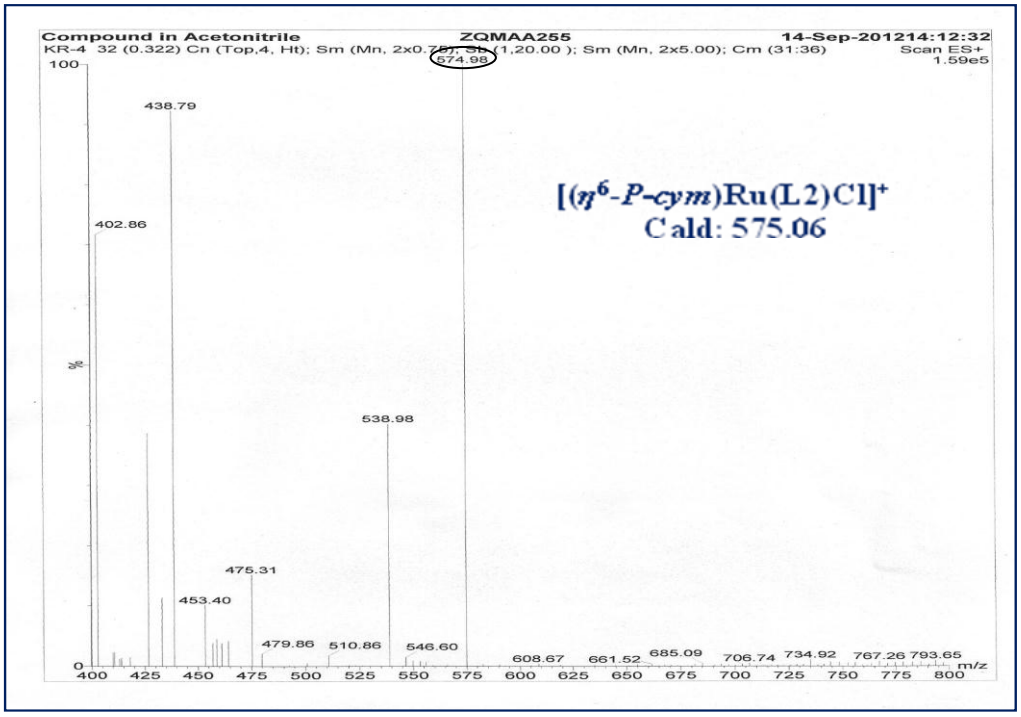

Figure S1. ESI-MS spectra of [Ru(η^6- *p*-cymene)(L2)Cl]$^+$ **4** in acetonitrile.

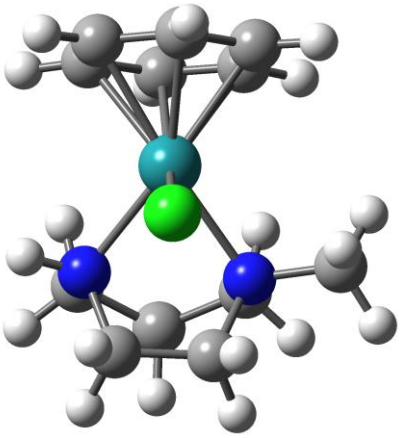

[Ru(η^6-benzene)(L1)Cl]$^+$ **1**

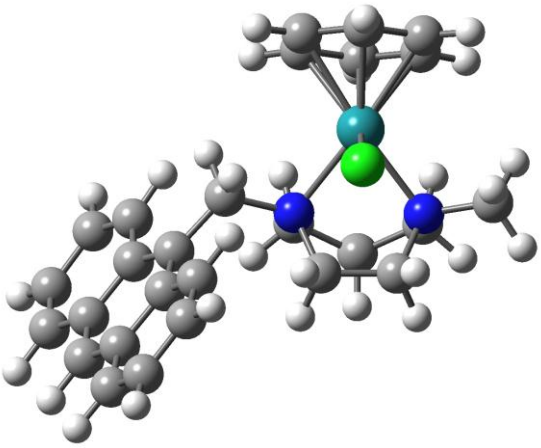

[Ru(η^6-benzene)(L2)Cl]$^+$ **2**

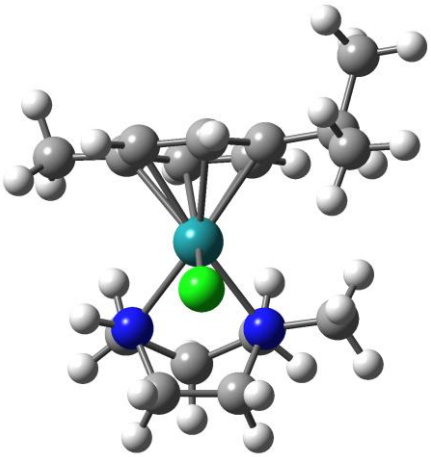

[Ru(η^6-*p*-cymene)(L1)Cl]$^+$ **3**

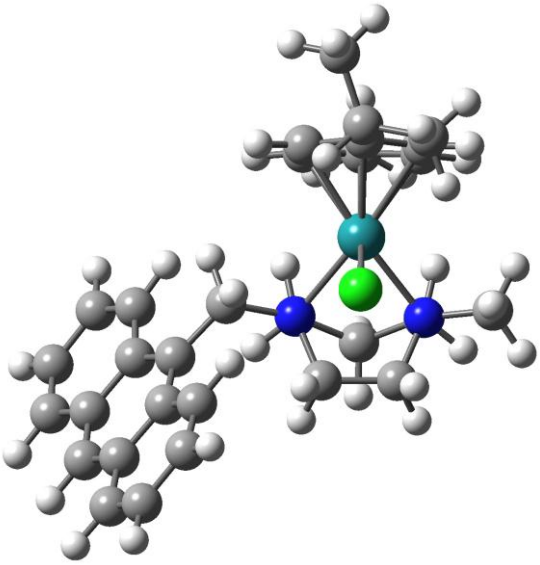

[Ru(η^6-*p*-cymene)(L2)Cl]$^+$ **4**

Figure S2. LANL2DZ and 6-31G(d,p) ground state optimized geometry of [Ru(η^6-benzene)(L1)Cl]$^+$ **1** , [Ru(η^6-benzene)(L2)Cl]$^+$ **2**, [Ru(η^6-*p*-cymene)(L1)Cl]$^+$ **3**, and [Ru(η^6- *p*-cymene)(L2)Cl]$^+$ **4.**

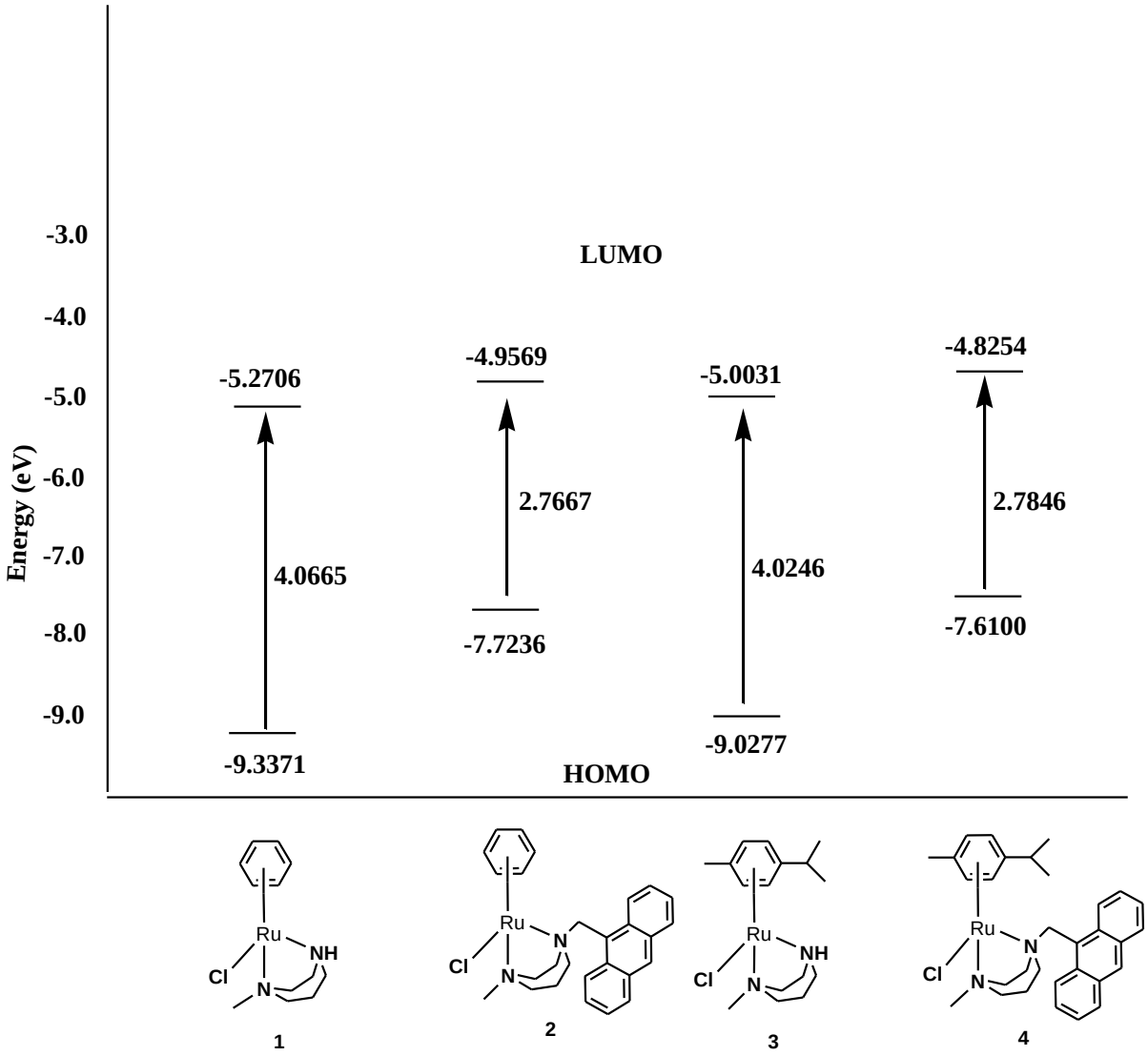

Figure S3. Ground state energy levels of the frontier molecular orbitals of complexes **1** – **4**.

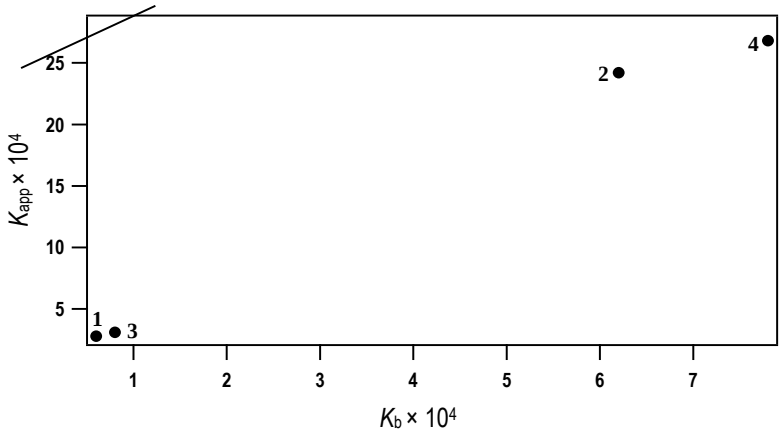

Figure S4. Plot of K_b vs K_{app} for **1** – **4**

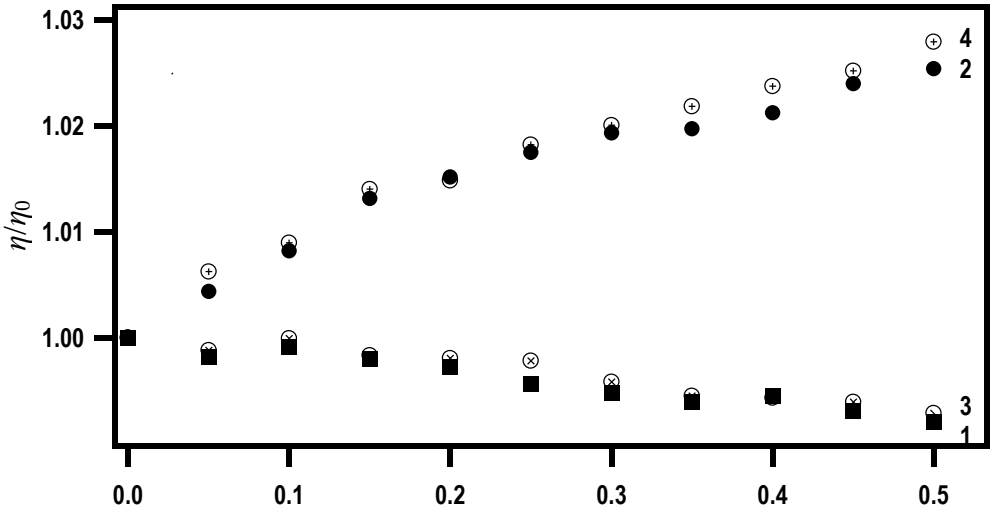

Figure S5. Effect of complexes **1** – **4** on the viscosity of CT DNA; relative specific viscosity *vs*.1/R; [CT DNA] = 500 μM.

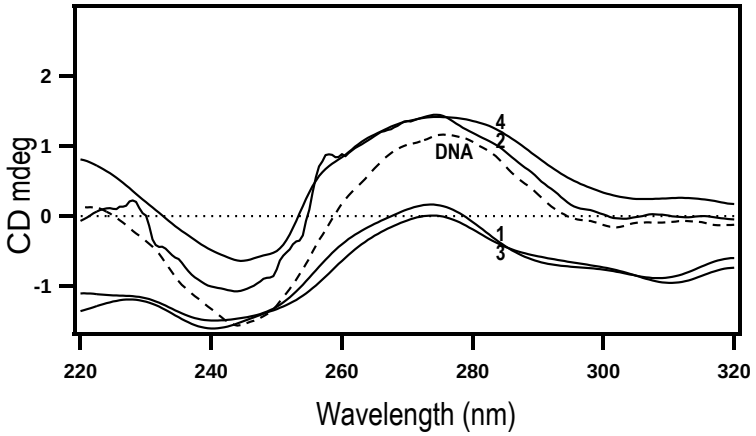

Figure S6. Circular dichroism spectra of CT DNA (2.5×10^{-5} M) in 5 mM Tris-HCl/50 mM NaCl buffer at pH 7.1 and 25^{o} C the absence (DNA) and presence of **1** – **4** at 1/R value of [Ru complex]/[DNA] =1.

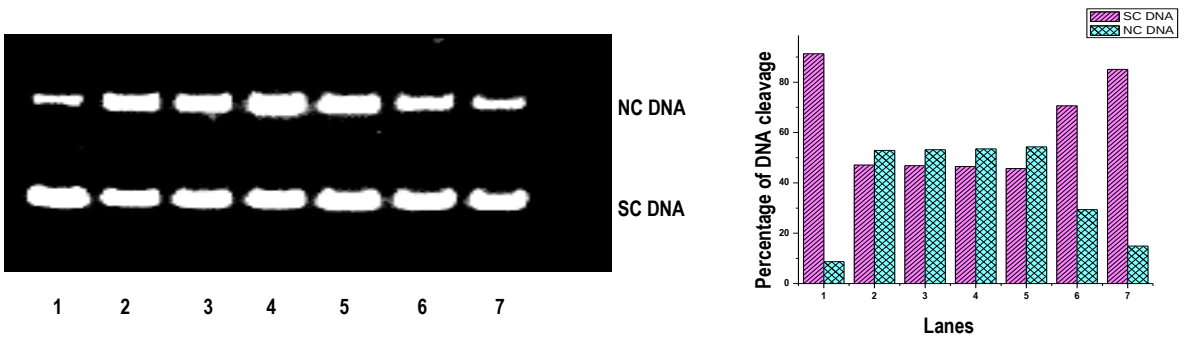

Figure S7. Cleavage of supercoiled pUC19 DNA (40 μM) by ruthenium(II) complexes **1** – **4** (150 μM) in absence of an external agent in a buffer containing 5 mM Tris HCl/50 mM NaCl at 37 ^{o}C. Lane 1, DNA; Lane 2, DNA + **1**; Lane 3, DNA + **2**; Lane 4, DNA + **3**; Lane 5, DNA + **4**; Lane 6, DNA + [Ru(η^6-*p*-cymene)Cl_2]$_2$; Lane 7, DNA + $RuCl_3 \cdot 3H_2O$. Forms SC and NC are Supercoiled and Nicked Circular DNA respectively. (B) Bar diagram showing the relative amounts of the different DNA forms in the presence of **1 – 4**.

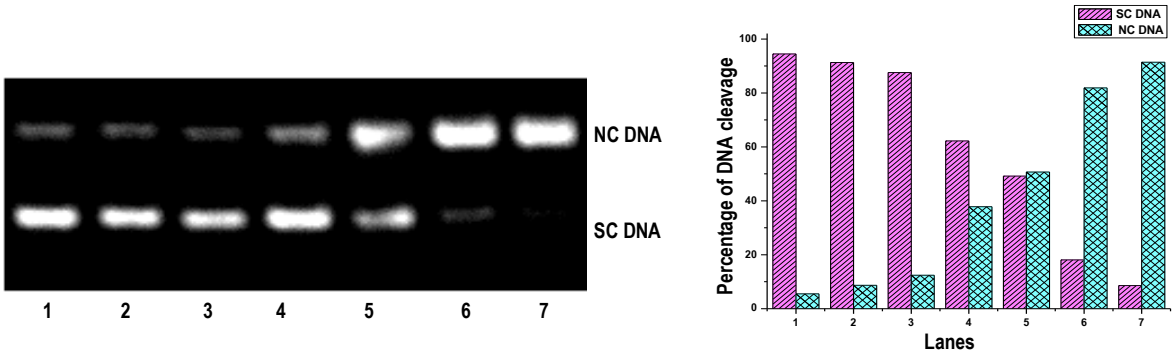

Figure S8. Concentration-dependent DNA (40 μM) cleavage by complex **4** (20 – 100 μM) in a buffer containing 5 mM Tris HCl/50 mM NaCl in the presence of H_2O_2 (30 μM) at 37 ^{o}C. Lane 1, DNA; Lane 2, DNA + H_2O_2 (30 μM); Lane 3, DNA + H_2O_2 + **4** (20 μM); Lane 4, DNA + H_2O_2 + **4** (40 μM); Lane 5, DNA + H_2O_2 + **4** (60 μM); Lane 6, DNA + H_2O_2 + **4** (80 μM); Lane 7, DNA + H_2O_2 + **4** (100 μM). SC and NC are supercoiled and nicked-circular forms of DNA, respectively

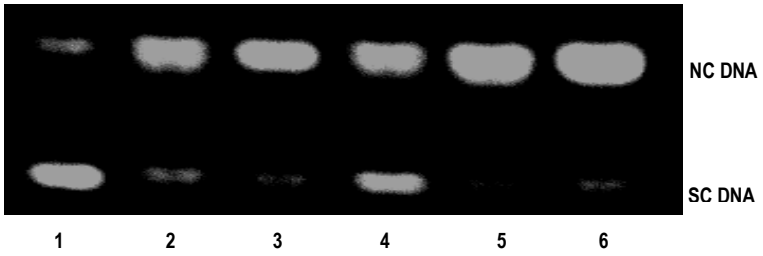

Figure S9. Mechanistic study of cleavage of the supercoiled pUC19 DNA (40 μM) by the complex **4** (100 μM) in a 5 mM Tris-HCl/50 mM NaCl at pH = 7.1 in the presence of various radical scavengers and in the presence of H_2O_2 (30 μM) at 37 ^{o}C for 1 h. Lane 1, DNA +

H_2O_2; Lane 2, DNA + H_2O_2 + **4** + NaN_3 (100 μM); Lane 3, DNA + H_2O_2 + **4** + Catalase (6 unit); Lane 4, DNA + H_2O_2 + **4** + DMSO (4 μL); Lane 5, DNA + H_2O_2 + **4** SOD (4 unit); Lane 6, DNA + H_2O_2 + **4**. Forms SC and NC is Supercoiled Nicked Circular DNA respectively.

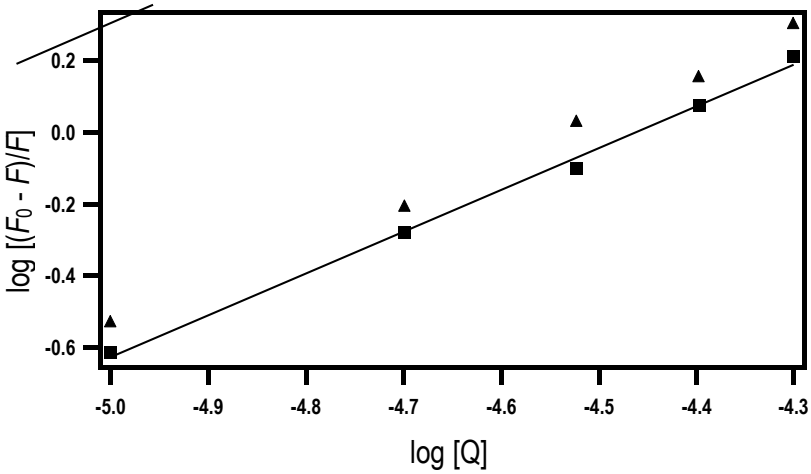

Figure S10. Plot of log [(F_0 - F)/F] vs log [Q] for **4** at 298 K(▲) and 308 K (■)

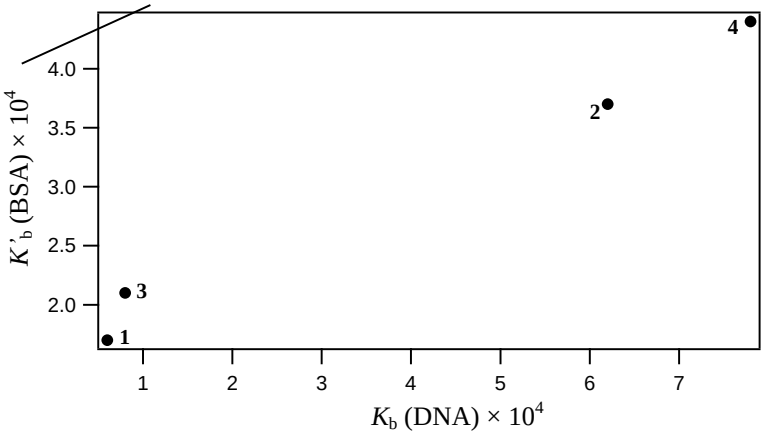

Figure S11. Plot of K_b (DNA) vs K'_b (BSA) for **1** – **4**

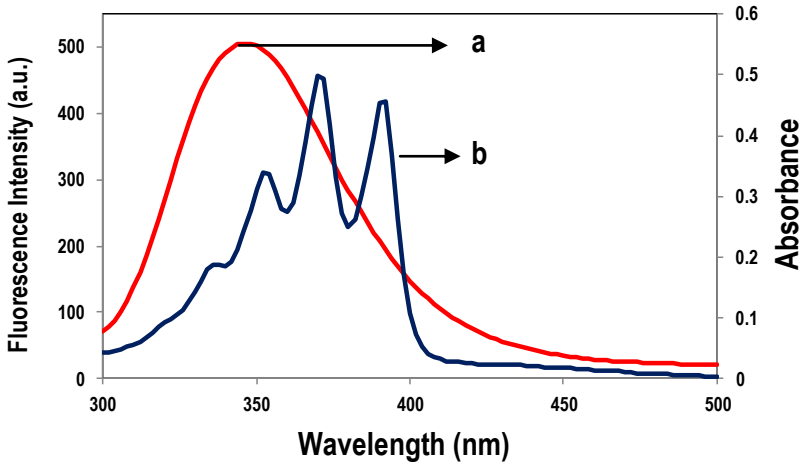

Figure S12 Overlap of the fluorescence spectra BSA (a) and the absorbance spectra (b) of **4**. [complex] = [BSA] = 1:1

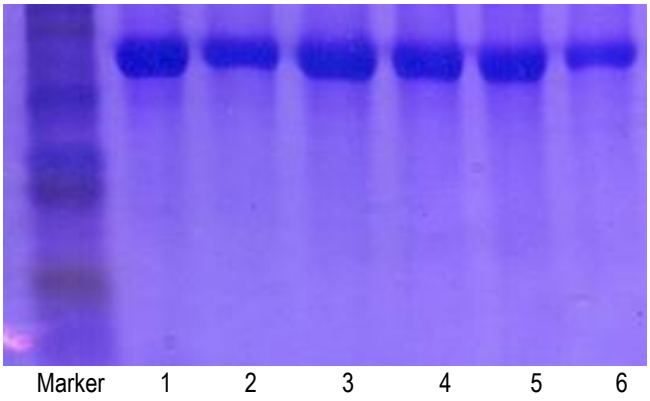

Figure S13. SDS-PAGE: BSA (15 μM) cleavage by ruthenium(II) complexes of **1** – **4** (500 μM) in phosphate buffer. Lane 1: BSA; Lane 2: BSA + [Ru(η^6-*p*-cymene)Cl_2]$_2$; Lane 3: BSA + **1**; Lane 4: BSA + **2**; Lane 5: BSA + **3**; Lane 6: BSA + **4**.

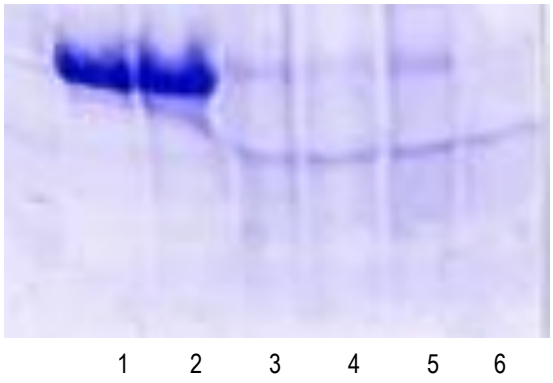

Figure S14. SDS-PAGE: BSA (15 μM) cleavage by ruthenium(II) complexes of **1** - **4** (500 μM) in presence of H_2O_2 (100 μM) in phosphate buffer. Lane 1: BSA; Lane 2: BSA + H_2O_2; Lane 3: BSA + **1** + H_2O_2; Lane 4: BSA + **2** + H_2O_2; Lane 5: BSA + **3** + H_2O_2; Lane 6: BSA + **4** + H_2O_2.